Optical phonon scattering of cavity polaritons in an electroluminescent device

A. Delteil,[1] A. Vasanelli,[1,*] P. Jouy,[1] D. Barate,[1] J. C. Moreno,[2] R. Teissier,[2] A. N. Baranov,[2] and C. Sirtori[1]

[1]*Laboratoire "Matériaux et Phénomènes Quantiques", Université Paris Diderot, CNRS UMR 7162, F-75013 Paris, France*
[2]*Institut d'Electronique du Sud, Université de Montpellier 2, F-34095 Montpellier, France*

A signature of the scattering between microcavity polaritons and longitudinal optical phonons has been observed in the electroluminescence spectrum of an intersubband device operating in the light-matter strong-coupling regime. By electrical pumping we resonantly populate the upper polariton branch at different energies as a function of the applied bias. The electroluminescent signal arising from these states is seconded by a phonon replica from the lower branch.

The strong coupling between light and matter in semiconductor microcavities gives rise to new quasiparticles, the microcavity polaritons.[1] Owing to their bosonic character, these particles can undergo stimulated scattering toward a final state[2] and give rise to a polariton laser.[3,4] One of the mechanisms that have been exploited for stimulated scattering is the optical phonon assisted relaxation, from an optically pumped excitonic reservoir into a minimum of the polaritonic dispersion curve.[5–7] Recently,[8] it was theoretically shown that optical phonons can be also at the origin of stimulated scattering of intersubband polaritons.[9] This scheme constitutes the basis for the realization of novel midinfrared lasers without electronic population inversion. In this Rapid Communication, we present an experimental signature of the scattering between intersubband polaritons and longitudinal optical (LO) phonons in an electrically injected quantum cascade device.[10] While electrons are resonantly injected in the upper polariton states only, the electroluminescence (EL) spectrum is composed of two features, from both branches, separated by the energy of an optical phonon. This scattering event shines light on the nature of the intersubband polaritons, in which the matter part interacts efficiently with the ions of the lattice, producing a profound variation of the photonic emission.

Our device is composed of a 20-period InAs/AlSb quantum cascade structure, imbedded into a planar microcavity. The latter consists of a top metallic mirror evaporated on the surface and a bottom reflector made of a doped InAs layer, as shown in the inset of Fig. 1. Each period of the cascade is based on a main well and an injection/extraction region, strongly doped to have a two-dimensional electron gas in the fundamental subband. The device is designed to ensure a light-matter strong-coupling regime between the $1 \rightarrow 2$ transition (at energy $E_{21} = 151$ meV) and the first-order mode of the planar microcavity. Angle-resolved multipass transmission experiments at 77 K were performed to characterize the structure. The energy position of the absorption maxima are plotted in Fig. 1 (squares) with respect to the in-plane photon wave vector $k_{||}$. They show a clear anticrossing between the intersubband transition and the cavity mode, with a vacuum field Rabi splitting of $2\hbar\Omega_R = 13$ meV. The absorption is simulated by using transfer matrix formalism (line): very good agreement with the experimental results is obtained by using an electronic density in the fundamental subband $N_s = 1.2 \times 10^{12}$ cm^{-2} (the nominal electronic density is 2×10^{12} cm^{-2}).

To perform angle-resolved EL spectra, the sample is etched into square mesas of 160 μm sides, mechanically polished, indium soldered onto a copper holder, and mounted in a cryostat. All the experimental results shown in this work were obtained at 77 K. The EL signal from the substrate was collected with a $f/2$ ZnSe lens, analyzed by a Fourier transform infrared spectrometer, and detected using a HgCdTe detector through a $f/0.5$ ZnSe lens. A schematized band diagram of the quantum cascade structure under applied bias is shown in Fig. 2(a). When the structure is aligned, electrons in the injector state can tunnel into subband 3 of the main quantum well. Electrons can then relax radiatively or nonradiatively (mainly by LO phonon emission) into subbands 2 and 1 in the main well. The extraction miniband ensures the electronic transport in the following period of the cascade. A very thin AlSb barrier (of nominal thickness 1 Å) is grown in the middle of the main well. The role of this barrier is to separate in energy the $3 \rightarrow 2$ and $2 \rightarrow 1$ transitions. In fact only wave functions corresponding to odd quantum numbers are modified by the presence of this barrier, which increases the energy of the $3 \rightarrow 2$ transition and reduces that of the $2 \rightarrow 1$ transition of the quantum well.[11] The dashed (blue) curve in Fig. 2(b) shows the EL spectrum measured at 8 V (at this voltage the injector is resonant with state 3) at 77 K, at an angle of 45°. At this angle the intersubband transition and the cavity mode are far from resonance,[12] allowing us to observe the bare intersubband transitions. The measured energies, $E_{21} = 154$ meV and $E_{32} = 214$ meV, are in very good agreement with the ones calculated with a three-band $\vec{k} \cdot \vec{p}$ model[13] by taking into account collective effects. (The simulated transition energies are $E_{21} = 151$ meV and $E_{32} = 213$ meV.) When the bias applied to the structure is reduced, the injector and subband 3 are not aligned anymore, and the intensity of the EL peak at energy E_{32} drops with respect to that at E_{21}, as shown in Fig. 2(b) by the (black) continuous curve, measured at 6 V. Note that in this case the EL spectrum presents a wide feature at energies between E_{21} and E_{32}. This is related to the diagonal transition between the injector state and subband 2, which is strongly dependent on the applied voltage.

By changing the detection angle, we investigate the regime in which the intersubband transition and the cavity mode are in resonance. Angle-resolved EL spectra measured at 6 V are shown in Fig. 2(c). The vertical lines give the energy position of the two bare transitions, as observed
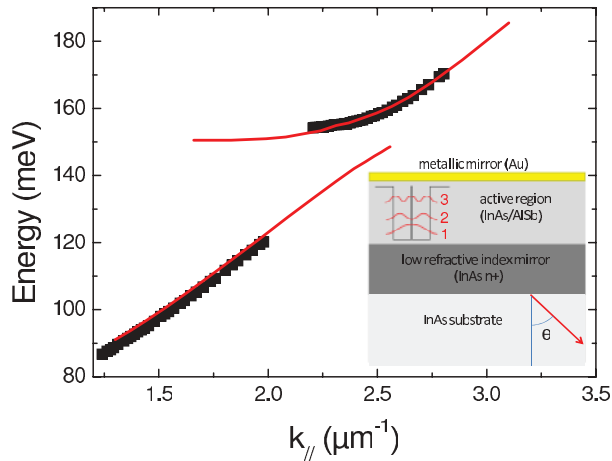
FIG. 1. (Color online) Measured and simulated polaritonic dispersion. Squares: absorption maxima measured at 77 K. Solid (red) line: absorption maxima simulated by transfer matrix. (inset) Schematic view of the sample. An InAs/AlSb quantum cascade structure is inserted in a planar microcavity, based on a metallic Au mirror and on a low-refractive-index InAs mirror. The structure is grown on a nonintentionally doped InAs substrate. θ is the internal angle for light propagation.

in Fig. 2(b). At low angles, the spectra are very similar to those observed at 45° because the system is far from the resonance condition. By increasing the internal angle of light propagation, we observe two peaks on both sides of E_{21}, whose energy position changes with the angle. We associate these peaks to EL features arising from the upper and lower polariton (respectively UP and LP) states. The third peak, at energy E_{32}, is not angle dependent: it is associated to a weak coupling between the $3 \rightarrow 2$ transition and the second-order cavity mode. It is important to notice that the two transitions in the main quantum well have very different behavior regarding their coupling with the cavity mode. In fact the vacuum Rabi energy is proportional to $\sqrt{N_g - N_e}$, where N_g (respectively N_e) is the electronic density of the ground (respectively excited) state of the transition. In our case only the fundamental subband is strongly populated, resulting in a strong coupling between the transition at E_{21} and the cavity mode. By comparing the spectra in Figs. 2(b) and 2(c), we can notice that the peaks associated to the upper polariton lie in the energy window corresponding to the transition between the injector and state 2. This is analogous to what was observed in other electroluminescent polaritonic devices,[10,12,14] where the injector resonantly populates the lower polariton branch. In the present case, the high conduction band discontinuity of the InAs/AlSb material system allows us to exploit the same mechanism to populate the polariton branches at higher energies. It is important to stress that this injection mechanism cannot be invoked to explain the observation of the peak associated to the lower polariton in the spectra of Fig. 2(c). Indeed the quantum cascade structure does not present any transition at this energy. The observation of the lower polariton branch is attributed to the relaxation of polaritons from the upper to the lower branch. This mechanism is represented in Fig. 3: the upper polariton branch is resonantly populated by the electronic injection, while the lower branch is populated
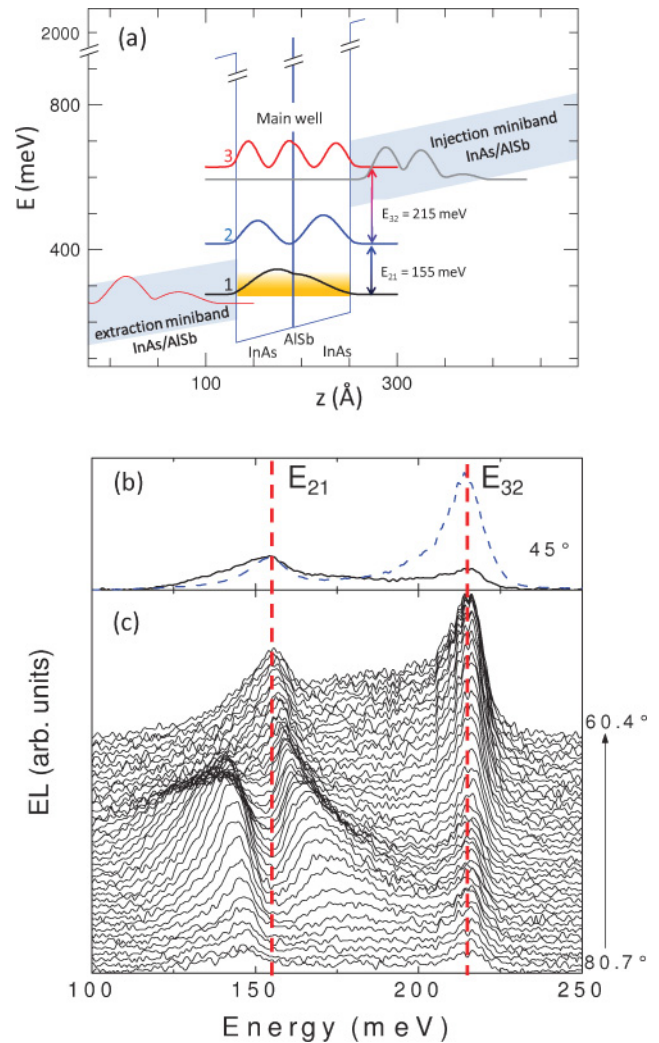

FIG. 2. (Color online) (a) Schematic band diagram of one period of the quantum cascade structure under an electric field of 70 kV/cm. The square moduli of the relevant wave functions are shown. The layer sequence of one period of the structure, in nm, starting from the main quantum well, is 5.9/**0.1**/5.9/**2.7**/5.5/**0.9**/5.2/**1.2**/5.0/ **1.2**/4.5/1/3.9/**1.2**/3.6/**0.9**/3.5/**1.2**/3.2/**0.9**/3.1/2. AlSb layers are in bold; italic layers are Te doped 1×10^{18} cm^{-3}. This sequence was repeated 20 times in the sample. (b) EL spectra measured at 45° internal angle at 8 V (600 mA, dashed line) and 6 V (58 mA, continuous line). (c) Angle-resolved EL spectra measured at 6 V.

thanks to the scattering between upper polaritons and LO phonons. This mechanism has been theoretically studied[8] in the presence of an optical pumping of the upper branch. It could lead to stimulated scattering of polaritons and to inversionless lasing. Figure 3 also presents a comparison between the polaritonic dispersion extracted from the angle-resolved EL spectra of Fig. 2(c) and that resulting from absorption spectra [see Fig. 1]. We can clearly see that the electroluminescent device allows us to observe the same polaritonic states as in absorption.

The EL spectra at different voltages are presented as contour plots in Fig. 4 (left-hand side). They have been normalized by the ratio between the detected optical power and the emitted one, which is a function of the Fresnel coefficients.[12] In these
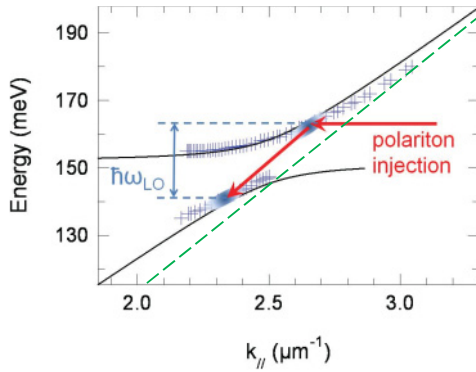
FIG. 3. (Color online) EL maxima (crosses) measured at 77 K and 6 V, compared with the polaritonic dispersion obtained in absorption (continuous line). The dashed line indicates the light cone. We also schematized the polariton population mechanism: electrical injection allows resonant pumping of the upper branch, while relaxation by LO-phonon emission allows the population of the lower branch.

graphs the EL intensity (color scale) is plotted as a function of the photon energy and in-plane wave vector ($k_{||}$) for different applied voltages (from top to bottom, 6, 5.5, and 4.7 V, respectively). At the three voltages, we can clearly see the EL signal associated to the two polariton branches, anticrossing at the energy of the intersubband transition (which slightly Stark shifts with the voltage, from 154.5 meV at 6 V to 151.5 meV at 4.7 V). In the three bias conditions, the energy difference between the maxima of the electroluminescence is close to 30 meV, which is the energy of a LO phonon in InAs. The comparison between the three panels shows that by changing
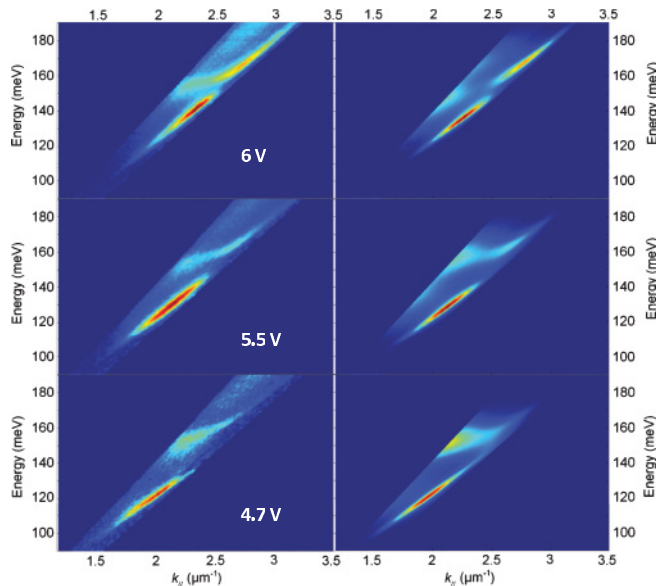

FIG. 4. (Color online) EL (color scale) measured at 77 K as a function of the photon energy and in-plane wave vector: (left) measured electroluminescence for 6 V (58 mA), 5.5 V (39 mA), and 4.7 V (22 mA); (right) simulated EL spectra for the corresponding voltages. We used the following parameters for the Gaussian functions: $\sigma = 9$ meV for the three voltages, while $E_{\rm inj}$ is equal to (top) 168 meV, (middle) 160 meV, and (bottom) 151 meV.

the bias applied to the device, the energy windows, in which the electroluminescence associated to the polariton branches is observed, are modified. In fact the UP is resonantly populated by the injector at an energy depending on the bias,[14] and the LP follows the same voltage dependence at an energy shifted by an LO phonon. Similar features are observed in the EL spectra up to room temperature.

The EL spectra are simulated as $\mathcal{L}_{\rm sim}(E,k_{||}) = A(E,k_{||}) \times n_{\rm occ}(E)$, where $A(E,k_{||})$ is the absorption spectrum of the device (i.e., the optical density of states), while $n_{\rm occ}(E) = n_{\rm UP}(E) + n_{\rm LP}(E)$ describes the occupation of the two polariton branches.[15] As the lower branch is populated by the relaxation of the upper polaritons, $n_{\rm LP}$ is proportional to $n_{\rm UP}$ via a coefficient depending on the upper and lower polariton energies, which are related to the voltage applied to the structure: $n_{\rm LP} = C(V) \times n_{\rm UP}$. This coefficient can also be expressed as the ratio between the radiative lifetime of the lower polariton (depending on the photonic Hopfield coefficient) and the polariton–LO phonon scattering time, which depends on the matter part of the initial and final states. In our simulation, analogously to Refs. [10] and [12], we model the occupation of the upper polariton by a Gaussian function $n_{\rm UP}(E) = \exp(-\frac{(E-E_{\rm inj})^2}{2\sigma^2})$, where $E_{\rm inj}$ is the injector energy and σ is its width; $n_{\rm LP}$ is described by an identical Gaussian function but centered at the energy $E_{\rm inj} - \hbar\omega_{\rm LO}$. The right-hand side of Fig. 4 shows the simulated EL spectra at the same voltages and in the same angular range as in the experiments. The simulated spectra reproduce very well all the experimental features: observation of the luminescence from both polariton branches and shift of the maxima of the electroluminescence with the voltage. The values $E_{\rm inj}$ and σ have been extracted from the low angle spectra.[12] For the three voltages, we found values of $C(V)$ of the order of unity (1.5, 2.3, and 1.5 from the highest to the lowest voltage). This means that the polariton–LO phonon scattering time is comparable with the lower polariton radiative lifetime (i.e., a few hundreds of femtoseconds). Furthermore, the lower polariton lifetime is limited by the radiative losses, and the intrabranch scattering is negligible.
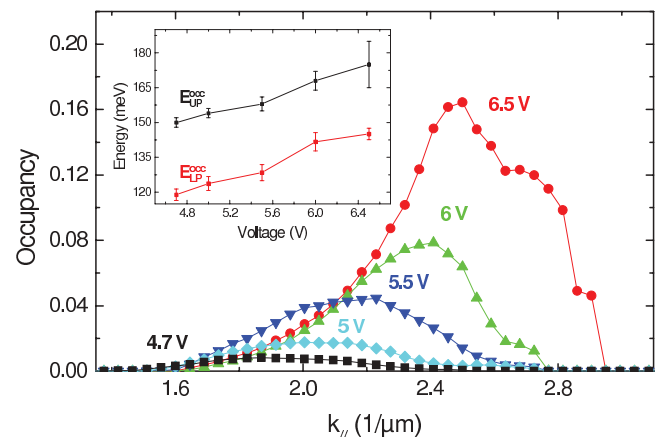

FIG. 5. (Color online) Lower polariton occupancy for different voltages. (inset) Energy evolution with the voltage of the LP and UP occupancy peaks. The mean value of the energy difference is 29.4 ± 1.8 meV, very close to the LO-phonon energy in InAs.

The excellent agreement between simulated and measured spectra is a proof that the emission of an LO phonon is the mechanism allowing the observation of the electroluminescence from the lower polariton branch. This interaction is considered by De Liberato and Ciuti[8] as a possible mechanism for polariton stimulated emission. As a consequence, by following Ref. [16], we estimate the occupation number for the lower polariton branch as a function of $k_{||}$ from the measured electroluminescence. We first estimate the power spectral density associated to the lower polariton branch after calibrating our HgCdTe detector. From this quantity, we deduce the LP density as a function of the in-plane wave vector by assuming that the radiative lifetime of a polariton state is inversely proportional to its photon fraction, which is the square modulus of the Hopfield coefficient associated to the photonic part. We found a LP density of the order of $\approx 8.5 \times 10^5$ cm^{-2} for the highest voltage. Because the density of states per unit surface is given by $dn/dk_{||} = k_{||}/(2\pi)$, we can deduce the occupancy of the LP branch, as a function of $k_{||}$. The results obtained for the different voltages are shown in Fig. 5 (main graph). The peak value of the occupancy increases linearly with the current by a factor of 20 in the considered range, reaching the value of approximately[17] $0.16^{+0.24}_{-0.03}$ at 6.5 V (98 mA). The error that we estimate on this value is mainly related to the cavity photon lifetime, which we took equal to 0.2 ps from our simulated absorption spectrum. For higher voltages, we do not observe an increase in the occupancy as the phonon scattering populates the lower polaritons outside the cone of light. From Fig. 5 (main graph), it is possible to see that the LP occupancy is, with good approximation, a Gaussian function of $k_{||}$ (up to 6 V), whose peak position shifts toward higher $k_{||}$ while increasing the voltage. In the interval where the energy varies linearly with $k_{||}$, this gives a Gaussian shape in energy for the LP occupancy, in agreement

with the model presented above. This Gaussian function has the same width (≈ 10 meV) as the one associated to the injector. Note that, when increasing the voltage, the occupancy curves become asymmetric. This is due to the proximity of the light cone (indicated by a dashed line in Fig. 3), which cuts off the electroluminescence signal for high $k_{||}$ values. The energies ($E_{\mathrm{LP}}^{\mathrm{occ}}$) corresponding to the peak occupancies at the different voltages are plotted in the inset of Fig. 5, together with the maximum of the occupancy of the UP branch ($E_{\mathrm{UP}}^{\mathrm{occ}}$), which is given by the energy position of the injector. The two occupancy maxima shift toward higher energies by increasing the voltage. The energy difference between them is (within the error) 30 meV, which is the energy of a LO phonon in InAs. This confirms that the occupancy of the LP is a phonon replica of that of the UP branch.

In conclusion, we provide evidence of intersubband polariton scattering with LO phonons. The signature of this effect is in the electroluminescence spectra, where two peaks separated by the energy of an optical phonon appear for different injection conditions. This process is realized by promoting electrons in the upper branch, at an energy which can be tuned with the voltage. Scattering with LO phonons populates the lower polariton branch, thus opening a new radiative path. Occupancy of 0.16 is observed for the lower polariton states. An increase of this value toward 1 would lead to stimulated emission[16] and laser without electronic population inversion. This could be readily obtained by decreasing the optical losses of the cavity and by modifying the polariton dispersion.[18]

---

*Angela.Vasanelli@univ-paris-diderot.fr

[1] C. Weisbuch, M. Nishioka, A. Ishikawa, and Y. Arakawa, Phys. Rev. Lett. **69**, 3314 (1992).

[2] P. G. Savvidis, J. J. Baumberg, R. M. Stevenson, M. S. Skolnick, D. M. Whittaker, and J. S. Roberts, Phys. Rev. Lett. **84**, 1547 (2000).

[3] S. Christopoulos, G. Baldassarri Höger von Högersthal, A. Grundy, P. G. Lagoudakis, A. V. Kavokin, J. J. Baumberg, G. Christmann, R. Butté, E. Feltin, J.-F. Carlin, and N. Grandjean, Phys. Rev. Lett. **98**, 126405 (2007).

[4] D. Bajoni, P. Senellart, E. Wertz, I. Sagnes, A. Miard, A. Lemaître, and J. Bloch, Phys. Rev. Lett. **100**, 047401 (2008).

[5] A. Imamoglu, R. J. Ram, S. Pau, and Y. Yamamoto, Phys. Rev. A **53**, 4250 (1996).

[6] F. Boeuf, R. André, R. Romestain, Le Si Dang, E. Péronne, J. F. Lampin, D. Hulin, and A. Alexandrou, Phys. Rev. B **62**, 2279 (2000).

[7] M. Maragkou, A. J. D. Grundy, T. Ostatnický, and P. G. Lagoudakis, Appl. Phys. Lett. **97**, 111110 (2010).

[8] S. De Liberato and C. Ciuti, Phys. Rev. Lett. **102**, 136403 (2009).

[9] D. Dini, R. Köhler, A. Tredicucci, G. Biasiol, and L. Sorba, Phys. Rev. Lett. **90**, 116401 (2003).

[10] L. Sapienza, A. Vasanelli, R. Colombelli, C. Ciuti, Y. Chassagneux, C. Manquest, U. Gennser, and C. Sirtori, Phys. Rev. Lett. **100**, 136806 (2008).

[11] J. Y. Marzin and J. M. Gérard, Phys. Rev. Lett. **62**, 2172 (1989).

[12] P. Jouy, A. Vasanelli, Y. Todorov, L. Sapienza, R. Colombelli, U. Gennser, and C. Sirtori, Phys. Rev. B **82**, 045322 (2010).

[13] C. Faugeras, A. Wade, A. Leuliet, A. Vasanelli, C. Sirtori, G. Fedorov, D. Smirnov, R. Teissier, A. N. Baranov, D. Barate, and J. Devenson, Phys. Rev. B **74**, 113303 (2006).

[14] Y. Todorov, P. Jouy, A. Vasanelli, L. Sapienza, R. Colombelli, U. Gennser, and C. Sirtori, Appl. Phys. Lett. **93**, 171105 (2008).

[15] R. P. Stanley, R. Houdré, C. Weisbuch, U. Oesterle, and M. Ilegems, Phys. Rev. B **53**, 10995 (1996).

[16] R. M. Stevenson, V. N. Astratov, M. S. Skolnick, D. M. Whittaker, M. Emam Ismail, A. I. Tartakovskii, P. G. Savvidis, J. J. Baumberg, and J. S. Roberts, Phys. Rev. Lett. **85**, 3680 (2000).

[17] The subscript and superscript indicate the error interval.

[18] Y. Todorov, A. M. Andrews, R. Colombelli, S. De Liberato, C. Ciuti, P. Klang, G. Strasser, and C. Sirtori, Phys. Rev. Lett. **105**, 196402 (2010).